Bioluminescence of the Largest Luminous Vertebrate, the Kitefin Shark, *Dalatias licha*: First Insights and Comparative Aspects

Jérôme Mallefet[1][†], Darren W. Stevens[2] and Laurent Duchatelet[1][†]*

[1] Marine Biology Laboratory, Earth and Life Institute, Université catholique de Louvain – UCLouvain, Louvain-la-Neuve, Belgium, [2] National Institute of Water and Atmospheric Research (NIWA), Wellington, New Zealand

Bioluminescence has often been seen as a spectacular yet uncommon event at sea but considering the vastness of the deep sea and the occurrence of luminous organisms in this zone, it is now more and more obvious that producing light at depth must play an important role structuring the biggest ecosystem on our planet. Three species of deepwater sharks (*Dalatias licha*, *Etmopterus lucifer*, and *Etmopterus granulosus*) were collected from the Chatham Rise, off New Zealand, and for the first time, we documented their luminescence. Comparison of glowing shark pictures, combined with histological description of light organs and hormonal control analysis, highlight the evolutive conservation of the bioluminescence process within Dalatiidae and Etmopteridae. A special emphasis is placed on the luminescence of *D. licha*, the largest known luminous vertebrate. This first experimental study of three luminous shark species from New Zealand provides an insight into the diversity of shark bioluminescence and highlights the need for more research to help understand these unusual deep-sea inhabitants: the glowing sharks.

Keywords: Dalatiidae, Etmopteridae, light emission control, photophore, shark

INTRODUCTION

Bioluminescence, defined as the production of visible light by living organisms, is a widespread phenomenon mainly encountered among various marine taxa (Widder, 1999; Haddock et al., 2010). This living light, also called cold light, occurs through a biochemical reaction; the oxidation of a substrate, a luciferin, by an enzyme, the luciferase, or through a stabilized complex called photoprotein (Shimomura, 2006). Among Squaliformes, bioluminescence is documented for two deep-sea families: Dalatiidae and Etmopteridae (Claes and Mallefet, 2009b; Straube et al., 2015). A third family, Somniosidae was recently suggested to also contain a luminous species, *Zameus squamulosus* (Günther, 1877), based on density and upper view of putative light organs (i.e., photophores) (Straube et al., 2015), new results brought clear evidence *Z. squamulosus* being a luminous species (Duchatelet et al., 2021). The first mentions of shark light emission date back to the nineteenth century (Bennett, 1840; Johann, 1899), but it is only recently that bioluminescence studies, focusing on physiological control, and photophore morphology and function, have been developed. These studies investigated bioluminescence in three etmopterids, *Etmopterus spinax* (Linnaeus, 1758), *Etmopterus molleri* (Whitley, 1939), *Etmopterus splendidus* (Yano, 1988), and one dalatiid, *Squaliolus aliae* (Teng, 1959) (e.g., Claes and Mallefet, 2009b,c, 2015; Claes et al., 2010a, 2011b, 2012; Renwart et al., 2014, 2015;

Duchatelet et al., 2019b, 2020b). Luminous sharks appear to produce blue-green light (between 455 and 486 nm; Claes et al., 2014a) for multiple purposes, such as counterillumination (Claes et al., 2010a), aposematism (Claes et al., 2013; Duchatelet et al., 2019b), and conspecific recognition (Claes et al., 2014a, 2015). Luminescence is achieved via thousands of photophores located within the epidermis. Each photophore is composed of a cup-shaped layer of pigmented cells encapsulating one to more than twelve photogenic cells (i.e., photocytes) and topped by one or more lens cells. In *E. spinax*, a guanine crystal reflector structure is located between the cup-shaped pigmented layer and the photocyte (Renwart et al., 2014, 2015). Photophores also display an iris-like structure (ILS), composed mainly of chromatophores, between the photocytes and the lens cells (Renwart et al., 2014; Duchatelet et al., 2020b). Recently, studies of the luminous system of *E. spinax* failed to identify the reactive compounds underlying the emission of light (i.e., luciferin/luciferase or photoprotein) (Renwart and Mallefet, 2013). Moreover, it has been demonstrated that shark luminescence is not due to symbiotic luminous bacteria (Duchatelet et al., 2019a). Therefore, the nature of the shark luminous system remains enigmatic.

In Metazoans, sharks are the only known bioluminescent organisms to hormonally control light emission. For the studied species, researchers have demonstrated the involvement of several hormones in the control of light emission: melatonin (MT) triggers light production, while alpha-melanocyte-stimulating (α-MSH) and adrenocorticotropic hormones (ACTH) inhibit it (Claes and Mallefet, 2009c; Duchatelet et al., 2020b). Prolactin triggers brighter and faster light emission than MT in Etmopteridae (Claes and Mallefet, 2009c; Claes et al., 2011b), while this hormone inhibits light production in *S. aliae* (Claes et al., 2012). More recently, *in silico* mRNA sequences and expression sites of MT and α-MSH/ACTH receptors were highlighted within the photophores, but neither mRNA sequences nor protein presence was found for the prolactin receptor (Duchatelet et al., 2020a). Other molecules, such as nitric oxide or γ-aminobutyric acid, also exhibited modulatory effects on light emission in some Etmopteridae (Claes et al., 2010b, 2011a). Finally, an extraocular opsin (Es-Opn3) has been demonstrated to be involved in a secondary control targeting the ILS and modulating the aperture of this pigmented structure acting as a light organ shutter (Duchatelet et al., 2020c). To establish the conservation of photophore morphology and the control of hormonal light emission in the evolution of luminous Squaliformes, increasing the knowledge on bioluminescent sharks is crucial.

While the majority of Squaliformes never reach more than 60 cm in adulthood, the kitefin shark (also named seal shark or black shark), *Dalatias licha* (Bonnaterre, 1788), can grow to 180 cm (Compagno, 1984; Roberts et al., 2015). This giant holobenthic dalatiid has a worldwide distribution at depths ranging from 50 to 1800 m but it is usually found in depths below 300 m (Compagno, 1984; Roberts et al., 2015). Recently, through baited-remote video and muscle enzymatic activity analysis, *D. licha* was suggested to be one of the slowest moving elasmobranch species (Pinte et al., 2020). Reif (1985) assumed that this shark is luminous as it presents pavement-like placoid

scales at the ventral side of the body like the related cookie cutter shark, *Isistius brasiliensis* (Quoy and Gaimard, 1824) (Reif, 1985; Widder, 1998; Delroisse et al., 2021). Nevertheless, no clear evidence has been put forward to confirm its luminescence status.

The diet of the kitefin shark is mainly composed of small demersal sharks such as lanternsharks (Etmopteridae), gulpersharks (Centrophoridae), and catsharks (Scyliorhinidae), followed by demersal fishes, crustaceans, and cephalopods (Macpherson, 1980; Matallanas, 1982; Dunn et al., 2010; Navarro et al., 2014). Chunks of large fast swimming epipelagic fishes have been also reported in the stomach contents of kitefin sharks (Matallanas, 1982), similar to what is observed for *I. brasiliensis* (Jones, 1971; Muñoz-Chápuli et al., 1988; Papastamatiou et al., 2010).

Along the coast of New Zealand, *D. licha* inhabit waters where at least six lanternshark species have been reported: *E. lucifer* (Jordan and Snyder, 1902), *E. granulosus* (Günther, 1880), *Etmopterus molleri*, *Etmopterus pusillus* (Lowe, 1839), *Etmopterus unicolor* (Engelhardt, 1912), and *Etmopterus viator* (Straube, 2011) (Roberts et al., 2015). Photophores have been observed for these species (Ohshima, 1911; Last and Stevens, 1994; Tracey and Shearer, 2002; Straube et al., 2011), but bioluminescence has only been confirmed for *Etmopterus molleri* (Claes and Mallefet, 2015). The blackbelly lanternshark (*E. lucifer*) and the southern lanternshark (*E. granulosus*) are the most common shark by-catch species in New Zealand deep-sea trawl fisheries (Blackwell, 2010). Studying light emission of the kitefin shark, the blackbelly lanternshark, and the southern lanternshark, might increase our understanding of their bioluminescence functions, and possible prey-predation relationships between these species.

Here, organization, morphology, density, and physiological control of kitefin shark photophores were investigated. To determine if this species displays the same photophore structure and hormonal control, a comparative analysis was performed on the two most abundant New Zealand lanternshark species, *E. lucifer* and *E. granulosus*. Results are compared to previously studied dalatiids and etmopterids. Homogeneity of light emission control among luminous elasmobranch and photophore structures among each shark families are observed, strengthening a conservative evolution of light emission capabilities among sharks. These observations and results raise questions on the luminescence role for the largest luminous vertebrate. The use of counterillumination for this giant luminous shark is here suggested to be co-opted for a camouflage-type approach as a predatory tool.

MATERIALS AND METHODS

Specimen Sampling

Shark specimens were captured during the Chatham Rise Trawl survey by the R.V. Tangaroa in January 2020 off the coast of eastern New Zealand. The survey used the same eight-seam hoki bottom trawl and survey methodology that was used on previous surveys (Hurst et al., 1992; Stevens et al., 2018). The net has 100 m

sweeps, 50 m bridles, 12 m backstrops, 58.8 m groundrope, 45 m headline, and 60 mm codend mesh. The trawl doors were Super Vee type with an area of 6.1 m^2.

The following depth range information are available: *D. licha* – mean maximal depth 678 ± 26 m (min-max 443–997 m); *E. lucifer* – mean maximal depth 542 ± 8 m [min-max 235–1078 m]; *E. granulosus* – mean maximal depth 903 ± 13 m (min-max 498–1269 m).

A total of 37 *D. licha* [40.9–138.0 cm total length (TL)], 304 *E. lucifer* (16.2–53.2 cm TL), and 281 *E. granulosus* (19.3–75.6 cm TL) were captured on the survey, of which 13 *D. licha*, 7 *E. lucifer*, and 4 *E. granulosus* were used for bioluminescence studies. Each specimen was maintained in a tank with fresh cold sea water in a dark cold room until manipulation. Each shark was sexed, measured, weighed (**Supplementary Table 1**) and photographed in dim daylight and in dark conditions using Sony α7SII camera before having a full incision of the spinal cord at the level of the first vertebrae, according to the European regulation for animal research handling. Ventral skin of a specimen of *S. aliae* and *I. brasiliensis*, collected, respectively, as in Delroisse et al. (2021) and Duchatelet et al. (2020b), were used for dalatiid comparative photophore histology.

Photophore Histology and Density

Skin patches of 3 cm^2 were dissected from different locations along the body of *D. licha* specimens (i.e., rostral, mandibular, pecto-ventral, pectoral, ventral, dorsal, dorsal fin, pelvic, flank, infra-caudal, precaudal, and caudal zones; **Figure 1A**) to assess photophore presence, size and densities. Skin patches were fixed in 4% formalin at least overnight before being transferred to phosphate buffer saline (PBS). Skin patches were observed and photographed under a transmitted light microscope (Leitz Diaplan, Germany) coupled with a ToupCam camera (UCMOS Series C-mount USB2.0 CMOS camera, ToupTek, Zhejiang, China). Photophore densities (per mm^2) and mean diameter (n = 30 or 50 zones per species) were also measured on the two etmopterid species using the same protocol (**Supplementary Figure 1**).

In parallel, skin patches of *D. licha*, *E. lucifer*, *E. granulosus*, *S. aliae,* and *I. brasiliensis* were used to perform histological sections across the photogenic organ. Skin tissues were bathed for 7 days in decalcifying solution (OsteoRAL, Fast decalcifier for Large Anatomical Specimens, RAL Diagnostics, France) with constant agitation and renewal of the solution every 2 days, rinsed in PBS, and placed in PBS with increasing concentrations of sucrose (10% for 1 h, 20% for 1 h, and 30% overnight). Tissues were then embedded in optimal cutting temperature compound (O.C.T. compound, Tissue-Tek, Netherlands) and rapidly frozen at −80°C. Sections of 10 μm were obtained with a cryostat microtome (CM3050S, Leica, Solms, Germany). Sections were placed on coated Superfrost slides (Thermo Scientific) and left overnight to dry. All sections were observed under a transmitted light microscope (Leitz Diaplan) equipped with a ToupCam camera (ToupTek).

Pharmacological Studies

In addition to the skin patches used for histology, round skin patches were dissected from the ventral luminous area of each shark using a metal cap driller (6 mm diameter) as described in Duchatelet et al. (2020b). Freshly dissected patches were rinsed and kept in shark saline [292 mmol L^{-1} NaCl, 3.2 mmol L^{-1} KCl, 5 mmol L^{-1} CaCl$_2$, 0.6 mmol L^{-1} MgSO$_4$, 1.6 mmol L^{-1} Na$_2$SO$_4$, 300 mmol L^{-1} urea, 150 mmol L^{-1} trimethylamine N-oxide, 10 mmol L^{-1} glucose, 6 mmol L^{-1} NaHCO$_3$; total osmolarity: 1.080 mOsmol; pH 7.7 (Bernal et al., 2005)] at 4°C in dark conditions before being used for pharmacological tests.

Hormones known to trigger or inhibit light emission in luminous elasmobranchs were applied (Claes and Mallefet, 2009c; Duchatelet et al., 2020b). Here, evaluations of the effect of MT, α-MSH and ACTH were conducted for the first time on the dalatiid species, *D. licha*, and the etmopterid species, *E. lucifer*, and *E. granulosus*.

Experiments were first conducted on 10 *D. licha* specimens. To obtain a dose response curve for MT application, three different concentrations of MT (i.e., 10^{-6}, 10^{-7}, 10^{-8} mol L^{-1}) were used. Skin patches were immersed in 200 μL of MT solution (either 10^{-6}, 10^{-7}, 10^{-8} mol L^{-1}). To analyze the effect of α-MSH and ACTH on the light emission of *D. licha*, another set of skin patches were subjected to an immersion in 100 μL of MT 10^{-6} mol L^{-1} followed after 5 min by an application of 100 μL of either α-MSH 10^{-6} mol L^{-1} or ACTH 10^{-5} mol L^{-1}. Luminescence of ventral skin patches subjected to the various treatments was measured using a FB12 tube-luminometer (Titertek-Berthold, Pforzheim, Germany) calibrated as in Duchatelet et al., 2020b. Lights emissions were recorded through FB12- Sirius, multiple kinetics software (Titertek-Berthold) for at least 30 min with a measurement every 58 s. For comparative purposes, similar treatments were performed on seven specimens of *E. lucifer* (same experiments) and four *E. granulosus* specimens (MT dose response and α-MSH treatments). In parallel, for *D. licha* and *E. lucifer*, photophore aperture and closure were observed after drug application by taking a time-lapse series of pictures (every 10 min) with a Sony α7SII camera mounted on a binocular microscope.

Luminescence measurements were characterized as follows (Duchatelet et al., 2020b): the maximum intensity of light emission [Lmax, in megaquanta per second (Mq s^{-1})], the total amount of light emitted during experimentation [Ltot, in Gigaquanta per hour (Gq h^{-1})] and the time to reach maximum light intensity [TLmax, in seconds (s)]. Inhibitory actions of α-MSH and ACTH were measured as the total amount of light emitted after the second drug application [Ltot$_{app}$, in Gq h^{-1}]. All light parameters were standardized according to the surface area of each skin patch (in cm^2). A second treatment (α-MSH or ACTH) was added to the first one when the light intensity plateau was reached with the MT application, each timing being species-specific. Results of the luminescence decrease were expressed as a percentage of the maximal luminescence value (i.e., plateau MT) measured before the second application.
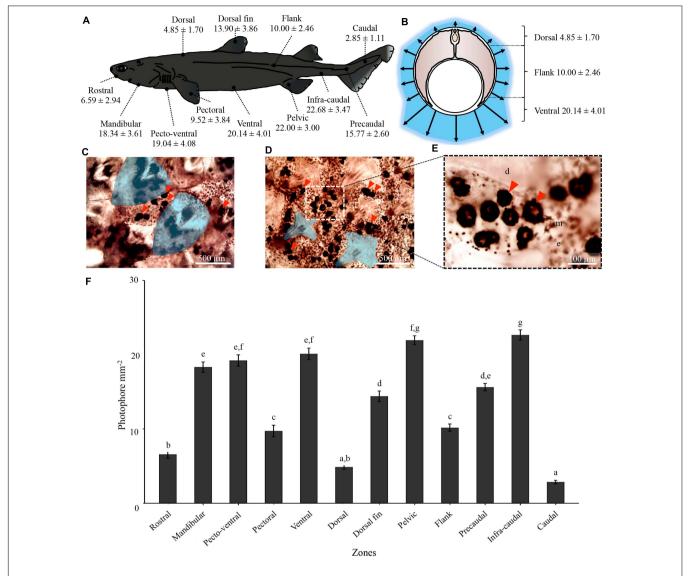
FIGURE 1 | *Dalatias licha* photophore visualization and density measurements. **(A)** Photophore densities for each studied zone along the shark body. **(B)** Representation of the dorso-ventral photophore density gradient. Black-dotted photophores (red arrowhead) observed between the placoid scales (delimited areas) at the **(C)** rostral and **(D)** ventral areas. Rostral area presents specific leaf-shaped placoid scales, while ventral area harbors typical pavement type placoid scales. **(E)** Close-up of the black circular-shaped photophores within the integument surrounding the ventral placoid scales. d, placoid scale; e, epidermis; m, melanophore; p, photophore. **(F)** Photophore density variation across the studied zones. Different lettering indicates statistical differences. All density values are expressed as mean ± SEM.

To evaluate the putative evolutive conservation of the hormonal control of light emission in dalatiids and etmopterids, pharmacological data on shark luminescence were extracted from literature.

Statistical Analyses

All analyses were performed with the software R studio (version 1.1.383, 2009, R Studio Inc., United States). Variance normality and homoscedasticity assumptions were tested by Shapiro-Wilk and Levene's test, respectively, before running ANOVA which reveals significant differences between skin photophore densities or pharmacological treatments. When these parametric assumptions were not met, a non-parametric Kruskal-Wallis ANOVA was used. *Post hoc* Tukey's tests or Wilcoxon tests allowed pair-wised comparison of means, attributing different letters to significantly different values (P-value < 0.05).

RESULTS

Luminous Pattern and Photophore Morphology

A blue glow was observed on the ventral surface of *D. licha*, *E. lucifer*, and *E. granulosus* specimens kept in a fully dark

environment (**Figures 2A,D,E**). *D. licha* also emit a faint blue glow from the lateral and dorsal areas and at the two dorsal fins (**Figure 3** – Mallefet personal observation). Both etmopterids present a more complex pattern of light emission with flank marks, and lateral, dorsal, and rostral patterns (**Figure 4**; *E. granulosus* – Mallefet personal observation). Skin patches observed *in toto* present black round-shaped

photophores distributed between placoid scales for all the observed sharks (**Figures 1C–E** and **Supplementary Figure 1**). The mean photophore diameters are 83.9 ± 9.5, 122.4 ± 10.8, and 132.3 ± 14.5 µm, for *D. licha*, *E. lucifer*, and *E. granulosus*, respectively. No statistical differences in photophore diameter were observed between the zones presenting large amount of photophores (ventral, pecto-ventral and infra-caudal) (*D. licha*
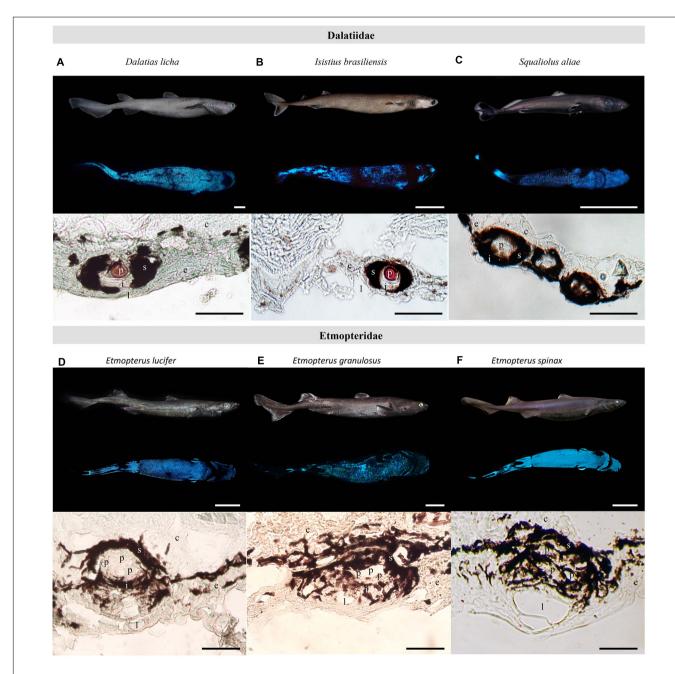

FIGURE 2 | Dalatiidae and Etmopteridae ventral luminous pattern and photophore histology. Picture of the lateral side in daylight, ventral luminescent pattern and section across ventral integument photophore of **(A)** *Dalatias licha*, **(B)** *Isistius brasiliensis*, **(C)** *Squaliolus aliae*, **(D)** *Etmopterus lucifer*, **(E)** *Etmopterus granulosus*, and **(F)** *Etmopterus spinax*. Ventral luminescence in dalatiid shows a homogenous pattern, while etmopterids show a heterogenous pattern with different zones. Photophores histology highlights a single photocyte within small photophores in dalatiids, while etmopterids harbor bigger and more complex photophores. c, connective tissue; e, epidermis; i, iris-like structure cells; l, lens cell; p, photocyte; s, pigmented sheath. *In toto* shark picture scale bar: 10 cm; photophore section scale bar: 100 µm.
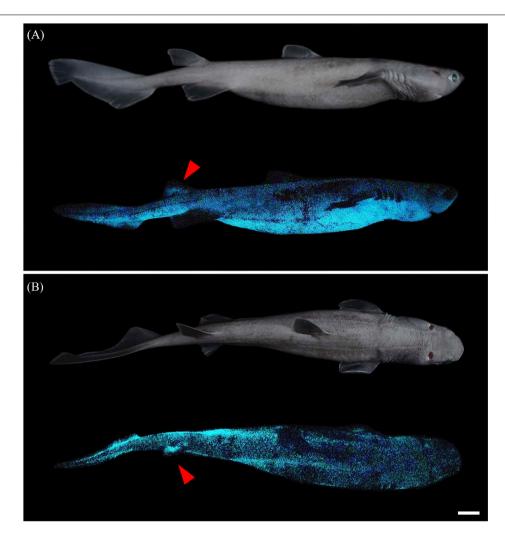
FIGURE 3 | Lateral and dorsal luminescent pattern of *Dalatias licha*. **(A)** Lateral daylight view and luminescent pattern highlighting the dorso-ventral luminous pattern. **(B)** Dorsal daylight view and luminescent pattern. Luminescence of the second dorsal fin is observable on this specimen (red arrowhead). Scale bar: 10 cm.

ANOVA: $F(2,183) = 1,1928$, P-value $= 0,3057$; *E. lucifer* ANOVA: $F(2,183) = 0,1014$, P-value $= 0,9036$; *E. granulosus* ANOVA: $F(2,183) = 0.1376$, P-value $= 0.8716$).

Analyses of photophore density along the *D. licha* body show an increasing dorso-ventral repartition of photophores reaching up to 20.14 ± 4.01 photophores per mm^2 at the ventral side of the shark (**Figures 1A,B,F**). The lowest densities were observed for the caudal and dorsal areas with a mean density of 2.85 ± 1.11 and 4.85 ± 1.70 photophores per mm^2, respectively (**Figure 1A**). Statistical differences [ANOVA: $F(11,514) = 128.64$, P-value $< 2.2 \times 10^{-16}$] in photophore densities are illustrated **Figure 1F** and **Supplementary Table 2A**. The scales of the rostral area were leaf-like in shape while the scales of the remaining body parts were pavement-like in shape (**Figures 1C,D**).

For both studied etmopterids, a high density of photophores was observed at the pectoral zone with 34.00 ± 6.20, and 15.63 ± 2.50 photophores per mm^2 for *E. lucifer* and *E. granulosus*, respectively. *E. granulosus* also have a high density of photophores at the infra-caudal and caudal zones.

Conversely, for both species, only a few photophores were spread within the dorsal epidermis. Both species have a well-defined flank mark with photophores. All the remaining photophore densities and their respective statistical differences [*E. lucifer* ANOVA: $F(9,490) = 263.39$, P-value $< 2.2 \ 10^{-16}$; *E. granulosus* ANOVA: $F(10,298) = 175.16$, P-value $< 2.2 \ 10^{-16}$] are reported in **Supplementary Figure 1** and **Supplementary Tables 2B,C**. Both etmopterids present needle-shaped placoid scales in all the studied zones (**Supplementary Figure 1**).

Histological sections across photogenic skin highlight the structure of *D. licha* photophores. Each light organ is embedded in the stratified squamous epidermis and is composed of a cup-shaped pigmented sheath containing a unique photocyte, topped by a lens cell with a few diffuse pigmented cells between the photocyte and lens cell (**Figure 2A**). This structural organization is similar to that found in *S. aliae* and *I. brasiliensis* photophores (**Figures 2B,C**).

Photophore morphologies of *E. lucifer* and *E. granulosus* are consistent with those already described for other etmopterids
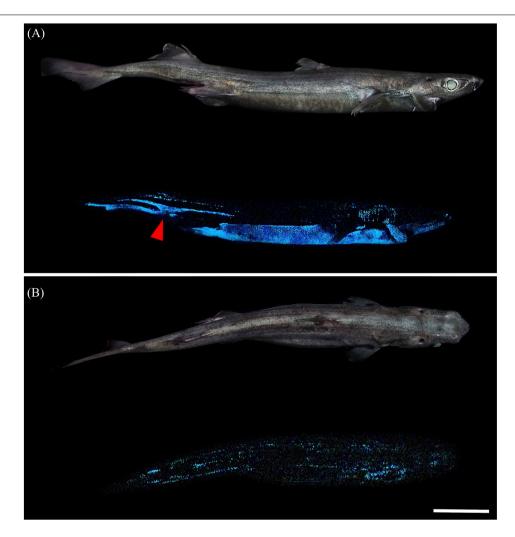
FIGURE 4 | Lateral and dorsal luminescent pattern of *Etmopterus lucifer*. **(A)** Lateral daylight view and luminescent pattern. The species-specific flank mark is indicated by a red arrowhead **(B)** dorsal daylight view and luminescent pattern with specific luminous lines. Scale bar: 10 cm.

(i.e., *E. spinax*, *Etmopterus molleri*, and *Etmopterus splendidus*) (**Figures 2D–F**). They are composed of a cup-shaped pigmented sheath embedded with luminous cells and topped a with lens. They are similar to dalatiid photophores, but they harbor a higher number of photocytes, a larger iris-like structure area, and more lens cells (up to 3) (**Figures 2D–F**).

Light Emission Control

The effect of MT on *D. licha*, *E. lucifer*, and *E. granulosus* was tested through a dose-dependent response. For the studied species, MT 10^{-6} mol L^{-1} triggered a long-lasting light emission, significantly different from the MT 10^{-8} mol L^{-1} application (*P*-value < 0.05; **Figures 5A–C** and **Supplementary Tables 3A, 4**), while MT 10^{-7} mol L^{-1} triggered an intermediate light emission and Ltot value (**Figures 5A–C** and **Supplementary Tables 3A, 4**). All treatments were significantly different from the shark saline control, except for the MT 10^{-7} and 10^{-8} mol L^{-1} treatments of *E. granulosus* (*P*-value < 0.05; **Supplementary Tables 3A, 4**). Although the total amount of light emitted under

MT 10^{-6} mol L^{-1} treatment was significantly different [Kruskal-Wallis $\chi^2(2)$ = 10.14, *P*-value = 0.0063], *E. lucifer* produced a mean total amount of light during the experiment 2.5 and 5 times higher than *D. licha* and *E. granulosus*, respectively. Similar patterns of bioluminescence were observed for the three species (**Figures 2, 5**).

The effect of α-MSH was evaluated for the three species after reaching the Lmax triggered through MT 10^{-6} mol L^{-1} application. Application of α-MSH 10^{-6} mol L^{-1} induced a rapid decrease of light emission for the studied luminous sharks (**Figures 6A–C** and **Supplementary Table 3B**). After MT-induced bioluminescence, Ltot$_{app}$ values of α-MSH were statistically significant compared with the MT 10^{-6} mol L^{-1} control (**Figures 6A–C** and **Supplementary Tables 3B, 5**).

The effect of ACTH was evaluated on *D. licha* and *E. lucifer* bioluminescence. Similar to the results obtained for α-MSH, ACTH 10^{-5} mol L^{-1} applications rapidly induced a decrease in light emission (**Figures 6A,B** and **Supplementary Table 3B**).
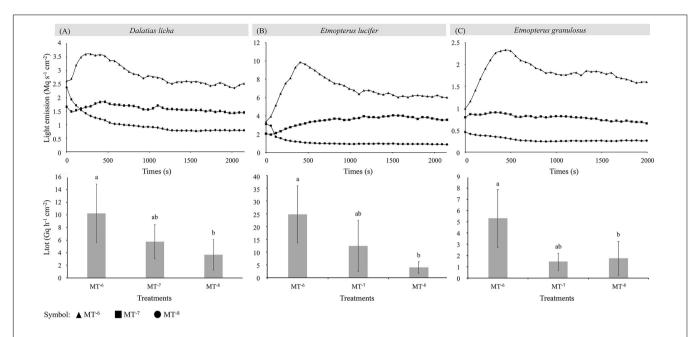
FIGURE 5 | Effect of MT on the studied species luminescence. Time course of the mean light emissions (Mq s^{-1} cm^{-2}) and total amount of light produced (Gq h^{-1} cm^{-2}) from ventral skin patches under hormonal treatments (MT 10^{-8} to 10^{-6} mol L^{-1}) for **(A)** *Dalatias licha* (n = 10), **(B)** *Etmopterus lucifer* (n = 7), and **(C)** *Etmopterus granulosus* (n = 4). Different lettering indicates statistical differences [Kruskal-Wallis ANOVA: *D. licha* χ^2(3) = 23.95, P-value = 2.56 × 10^{-5}; *E. lucifer* χ^2(3) = 23.823, P-value = 2.72 × 10^{-5}; *E. granulosus* χ^2(3) = 8.5368, P-value = 0.0361]. Error bars correspond to SEM.
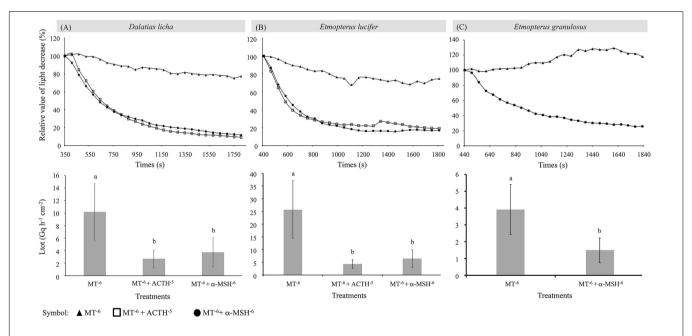

FIGURE 6 | Effect of ACTH and α-MSH on luminescence induced by MT in the studied species. Time course of the light produced (expressed as percentage of maximal melatonin control value), and total amount of light produced (Gq h^{-1} cm^{-2}) after melatonin pretreatment from ventral skin patches under melanocortin treatments (ACTH 10^{-5} mol L^{-1}/α-MSH 10^{-6} mol L^{-1}) for **(A)** *Dalatias licha* (n = 10), **(B)** *Etmopterus lucifer* (n = 7), and **(C)** *Etmopterus granulosus* (n = 4 – no ACTH treatment). Hormonal treatments are expressed in mol L^{-1}. Different lettering indicates statistical differences [ANOVA: *D. licha* $F_{(2,33)}$ = 2.585, P-value = 0.0437; *E. lucifer* $F_{(2,18)}$ = 14.482, P-value = 0.0002; Kruskal-Wallis ANOVA: *E. granulosus* χ^2(1) = 3.857, P-value = 0.0495]. Error bars correspond to SEM.

Each Ltot$_{app}$ value of ACTH 10^{-5} mol L^{-1} was not significantly different from those of α-MSH 10^{-6} mol L^{-1}, respectively, but were statistically different from the MT 10^{-6} mol L^{-1} control (**Figures 6A,B** and **Supplementary Tables 3B, 5**). Mean values of Lmax, TLmax, Ltot, Ltot$_{app}$ are presented in **Supplementary Table 3**.

The time-course of light emission in *D. licha* under MT 10^{-6} mol L^{-1} stimulation revealed a concomitant opening of the photophore ILS within 15 min of luminescence, in which the ILS stayed open for the next 30 min while the light level remained high (**Figure 7A**). In the case of *E. lucifer* MT-induced luminescence, a rapid opening of the photophore ILS was observed within 8 min followed by a slow decrease during which a closure of the ILS was visible (**Figure 7B**). Aperture and closure of photophores showed pigment movements concomitant to light emission.

DISCUSSION

The three studied shark species inhabit the mesopelagic zone (Roberts et al., 2015), therefore they face an environment with
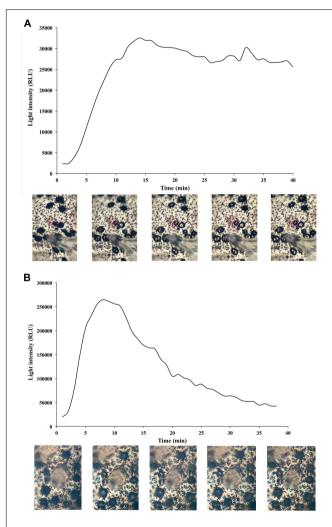

FIGURE 7 | Time-course of MT-induced luminescence, and time-lapse of photophore pigment movements. Luminescence in relative light unit (RLU) recorded during a 40 min MT 10^{-6} mol L^{-1} application on ventral skin patches and time-lapse pictures (times: 0, 10, 20, 30, and 40 min, respectively) of photophore pigment movements of **(A)** *Dalatias licha*, **(B)** *Etmopterus lucifer*.

no place to hide, hence the need for glowing camouflage or counterillumination, first proposed by Clarke, 1963. The mesopelagic zone, often called the twilight zone, ranges from 200 to 1000 m depth (maximal depth of solar light penetration) and is the realm of bioluminescence (Martini and Haddock, 2017; Martini et al., 2019). At 200 m the residual solar light is considered too weak to initiate photosynthesis but organisms living there are well adapted to see in low light conditions (Nicol, 1978). Mesopelagic cephalopods, sharks and bony fishes have large eyes with specialized structures such as a large iris, a tapetum, huge rod density, high content of opsins (rhodopsin and chrysopsin), and an elevated integration rate at the optical nerve which allows them to perceive very low light levels down to 800 m depth (Douglas et al., 1998; Warrant, 2004; Warrant and Locket, 2004; Claes et al., 2014a,b).

Luminescent Pattern

The light emission pattern observed in *D. licha* is similar to that observed in previously studied dalatiids i.e., *S. aliae* and *I. brasiliensis* (Claes et al., 2012; Delroisse et al., 2021). The dorso-ventral gradient and the relative homogeneity in ventral photophore densities suggest the luminescence is used for counterillumination. The luminous pelvic zone of *D. licha* reveals a sexual dimorphism but, contrary to *E. spinax* and *Etmopterus molleri* (Claes and Mallefet, 2010b; Duchatelet et al., 2020c), it is not brighter than the rest of the ventral body, suggesting it is less important for sexual signaling. The kitefin shark *D. licha,* like other dalatiids, does not have flank marking or specific dorsal patterns. The lack of these luminescent patterns, previously suggested to be used as conspecific signaling for group aggregation, swimming, or hunting in etmopterids (Claes et al., 2015; Duchatelet et al., 2019b), rules out this function in *D. licha*. The aposematic function described for etmopterids (Claes et al., 2013; Duchatelet et al., 2019b) is also ruled out for *D. licha* luminescence due to the absence of dorsal fin defensive spines. Nevertheless, *D. licha* is the first shark with fully luminous dorsal fins (**Figures 1A**, **3**), which raises questions about its luminescence function.

The light emission patterns of *E. lucifer* and *E. granulosus*, are similar to that of previously studied etmopterids. The dorsal photophores, flank markings, and brighter pectoral fin and claspers are likely to be used for intraspecific communications while the ventrally emitted light is likely to be used for counterillumination. These functions have been documented for *E. spinax* (Claes and Mallefet, 2009a; Claes and Mallefet, 2010a), *Etmopterus molleri* (Claes and Mallefet, 2015), and *Etmopterus splendidus* (Claes et al., 2011b). However, a bioluminescence aposematic function through specific spine-associated photophores (Claes et al., 2013; Duchatelet et al., 2019b) was not documented for *E. lucifer* and *E. granulosus*.

Reif (1985) postulated that a trade-off exists between the space occupied by placoid scales and luminous organs, and that four different types of placoid scales have evolved to allow this trade-off: pavement, cross-, bristle/ needle-, and hook-shaped placoid scales. A new type of squamation with overlapping leaf-shaped placoid scales is present in the luminous rostral area of *D. licha*. This new bioluminescent-associated squamation

was observed in the somniosid, *Zameus squamulosus*, which is assumed to be luminous (Straube et al., 2015). This new type of bioluminescence-associated placoid scale needs to be highly translucent or possess specific physical characteristics to allow efficient light transmission. The use of Reif placoid scale types to assess the bioluminescent status of a shark species is not a decisive character as shown by a recent study of Ferrón et al. (2018); highlighting the presence of bioluminescent-like squamation in a galeomorph shark, *Apristurus ampliceps*, a species not known to be luminous.

Photophore Morphology Conservation

Histology revealed an evolutive conservation of photophore morphology across each family. Kitefin shark photophores are larger (mean diameter 83.9 µm) than those observed in *S. aliae* and *I. brasiliensis* [i.e., 50 and 56 µm, respectively (Claes et al., 2012; Delroisse et al., 2021)] while the internal structure of typical dalatiid photophores is conserved. Here, *D. licha* photophores are depicted as morphologically similar to those of *S. aliae, S. laticaudus* and *I. brasiliensis* (Seigel, 1978; Delroisse et al., 2021).

E. lucifer and *E. granulosus* showed typical etmopterid photophore histology (Claes and Mallefet, 2009b, 2015; Claes et al., 2011b; Renwart et al., 2014; Duchatelet et al., 2020b). These observations provide further insights on the evolutive conservation of light organ morphology across luminous squaliform radiation (Straube et al., 2015).

Luminescence Control Evolutive Conservation

The effect of hormones on light emission in *D. licha, E. lucifer* and *E. granulosus* are consistent with increasing literature on light emission control in sharks (Claes and Mallefet, 2009c; Claes et al., 2012; Duchatelet et al., 2020b,d): MT, and α-MSH/ACTH, have been demonstrated as the main triggering and inhibiting agents of shark luminescence, respectively. Similar to observations of *E. spinax* and *Etmopterus molleri* photophores (Claes and Mallefet, 2010a; Duchatelet et al., 2020b), aperture and closure of *D. licha* and *E. lucifer* photophores involved pigment motion within the ILS cells. Simultaneities of curves kinetics and pigment motions highlight the evolutive conservation of hormonally controlled pigment motion regulating luminescence. These data strongly suggest that luminous etmopterids and dalatiids share a common luminescence control mechanism, involving at least MT, and α-MSH/ACTH hormones. This control is assumed to have been successfully and evolutionary co-opted from shark melanophore pigment motion control by a common ancestor of these two squaliform families. For both families, luminescence appears to be dually controlled at the level of (*i*) the photocyte, site of luminescent reaction, and (*ii*) the ILS cells, acting as a diaphragm capable of occluding light produced by the photocytes, via melanophore-associated pigment movements (Duchatelet et al., 2020b,d). This was recently demonstrated within ILS cells of the lanternshark, *E. spinax* (Duchatelet et al., 2020d) i.e., transduction pathways that activate cellular motors such as dynein and kinesin, leading pigment movements within ILS melanophores. The bioluminescence control mechanisms

in the two studied etmopterids, as well as in *D. licha*, might share common features. Moreover, the involvement of extraocular photoreception events in the light emission control of photophores (Duchatelet et al., 2020d), remains to be deciphered for these sharks. Further research are necessary to fully demonstrate the evolutive conservation of luminescence control within etmopterids and dalatiids.

Luminescence of *Dalatias licha*

The question remains concerning bioluminescence in the largest luminous vertebrate; why does *D. licha* emit light ventrally to counterilluminate when it has few or no predators? Pinte et al. (2020), analyzed the swimming speed of several New Zealand deep-sea sharks, and found that *D. licha* possesses one of the slowest cruise swimming speeds ever measured in sharks. Conversely, this species is assumed to possess a high burst capability (Pinte et al., 2020). Stomach content analyses have revealed that this shark species hunts and eats etmopterids, which have a higher cruise swimming speed. Therefore, there are two hypotheses which might explain the ventral luminescence of this holobenthic species: luminescence might be used (*i*) to illuminate the ocean floor while searching and hunting for prey; or (*ii*) to stealthily approach toward prey, using counterillumination camouflage, before striking fast when close enough (Zintzen et al., 2011), allowing them to predate etmopterids. In both cases, the principle of counterillumination would have been distorted to serve as a predation tool instead of an avoidance mechanism, a hypothesis already proposed for the cookie cutter shark, *I. brasiliensis* (Widder, 1998). However, to validate such hypotheses for these dalatiid species, *in vivo* observations and behavioral studies are essential.

CONCLUSION

Through a histological and pharmacological approach, the bioluminescence of three different shark species was investigated. Our results support evolutive conservation of light organ morphology and luminescence control. For the first time, luminescence was recorded and analyzed for the largest luminous vertebrate, *D. licha* and two lanternsharks, *E. lucifer* and *E. granulosus*. Dalatiid photophores are similar between species and are structurally composed of a single photocyte embedded in a cup-shaped pigmented cell and surmounted by lens cells. The same observation was made for etmopterids, which showed a conservation of photophore structure between species. Etmopterid photophores are slightly more complex than those of dalatiids, with several photocytes and a well-developed ILS between the lens cells and the photocytes. Through this study, the action of MT and α-MSH/ACTH in the bioluminescence control in these two families was shown to be identical and seem to have been co-opted during evolution from the regulation of skin pigment movements. With these data, we can assume that the common luminous ancestor of etmopterids and dalatiids likely had hormonal control of its luminescence and had luminous organs similar to those of the dalatiids (i.e., the simplest structure) for counterillumination.

DATA AVAILABILITY STATEMENT

The original contributions presented in the study are included in the article/**Supplementary Material**, further inquiries can be directed to the corresponding author/s.

ETHICS STATEMENT

Ethical review and approval was not required for this study. The shark specimens were captured as bycatch of a fisheries assessment survey for the New Zealand Ministry for Primary Industries.

AUTHOR CONTRIBUTIONS

JM and DS collected the samples. JM collected the bioluminescence pictures and performed pharmacological studies and fixations on the survey. LD performed the classical histology, pattern, and pharmacological analyses. LD and JM were major contributors to the initial manuscript that was improved by DS revisions. All authors approved the final manuscript.

FUNDING

ACKNOWLEDGMENTS

This study is the contribution BRC #276 of the Biodiversity Research Center (UCLouvain) from the Earth and Life Institute Biodiversity (ELIB) and the "Centre Interuniversitaire de Biologie Marine" (CIBIM).

SUPPLEMENTARY MATERIAL

The Supplementary Material for this article can be found online at: https://www.frontiersin.org/articles/10.3389/fmars.2021.633582/full#supplementary-material

Supplementary Figure 1 | External features and densities of photophores in *Etmopterus lucifer* and *Etmopterus granulosus*. Black-dotted photophores observed at the ventral side **(A)**, flank mark **(B)**, and pectoral **(C)** specific area of *E. lucifer*. Dotted line corresponds to the flank mark boundaries. **(D)** Measured photophore densities for the studied zones of *E. lucifer* ($n = 50$ for each zones). Black-dotted photophore observed at the ventral **(E)**, infra-caudal **(F)** and rostral **(G)** areas of *E. granulosus*. **(H)** Measured photophore densities for the studied zones of *E. granulosus* ($n = 30$ for each zones). Different lettering indicates statistical differences. Values are expressed as mean $\pm$ SEM. Scale bars: 750 μm.

Supplementary Table 1 | Experimental specimens. Morphometrics measurements of *Dalatias licha*, *Etmopterus lucifer*, *E. granulosus*, *Squaliolus aliae* and *I. brasiliensis* studied specimens. ♀, female; ♂, male.

Supplementary Table 2 | Photophore density, statistical analyses. Results of Tukey's test for the photophore density of **(A)** *D. licha,* **(B)** *E. lucifer,* and **(C)** *E. granulosus* different skin zones. Gray-shaded cases represent not significant differences.

Supplementary Table 3 | Hormone-induced luminescence parameters (mean maximal light intensity: Lmax; time to reach the Lmax: TLmax; total amount of emitted light: Ltot; total amount of emitted light after second drug application: Ltot$_{app}$). **(A)** luminescence recorded parameters for the melatonin (MT) dose response treatments for *Dalatias licha* ($n = 12$), *Etmopterus lucifer* ($n = 7$) and *E. granulosus* ($n = 4$). *indicate significant differences (P-value < 0.05) from the shark saline control experiment. **(B)** Ltot$_{app}$ for each treatment and each shark species. *indicate differences (P-value < 0.05) from the melatonin 10^{-6} mol L^{-1} control experiment. All data are means $\pm$ SEM.

Supplementary Table 4 | MT dose response, statistical analyses. Kruskal-Wallis ANOVA and pairwise Wilcoxon test results for the MT dose response of the three studied sharks. Gray-shaded cases represent not significant differences.

Supplementary Table 5 | α-MSH and ACTH effects, statistical analyses. ANOVA and Tukey's test results for the decrease of light triggered by α-MSH and ACTH treatments (except for *E. granulosus* non-parametric test). Gray-shaded cases represent not significant differences.

REFERENCES

Bennett, F. D. (1840). *Narrative of a Whaling Voyage Round the Globe, from the Year 1833 To 1836*, Vol. 2. Moscow: Рипол Классик.

Bernal, D., Donley, J. M., Shadwick, R. E., and Syme, D. A. (2005). Mammal-like muscles power swimming in a cold-water shark. *Nature* 437, 1349–1352. doi: 10.1038/nature04007

Blackwell, R. G. (2010). *Distribution and Abundance of Deepwater Sharks in New Zealand Waters, 2000–01 to 2005–06. New Zealand Aquatic Environment and Biodiversity Report No. 57*. Wellington: Ministry of Fisheries.

Claes, J. M., Aksnes, D. L., and Mallefet, J. (2010a). Phantom hunter of the fjords: camouflage by counterillumination in a shark (*Etmopterus spinax*). *J. Exp. Mar. Biol. Ecol.* 388, 28–32. doi: 10.1016/j.jembe.2010.03.009

Claes, J. M., Dean, M. N., Nilsson, D. E., Hart, N. S., and Mallefet, J. (2013). A deepwater fish with 'lightsabers' – dorsal spine-associated luminescence in a counterilluminating lanternshark. *Sci. Rep.* 3:1308. doi: 10.1038/srep01308

Claes, J. M., Ho, H.-C., and Mallefet, J. (2012). Control of luminescence from pygmy shark (*Squaliolus aliae*) photophores. *J. Exp. Biol.* 215, 1691–1699. doi: 10.1242/jeb.066704

Claes, J. M., Krönström, J., Holmgren, S., and Mallefet, J. (2010b). Nitric oxide in the control of luminescence from lantern shark (*Etmopterus spinax*) photophores. *J. Exp. Biol.* 213, 3005–3011. doi: 10.1242/jeb.040410

Claes, J. M., Krönström, J., Holmgren, S., and Mallefet, J. (2011a). GABA inhibition of luminescence from lantern shark (*Etmopterus spinax*) photophores. *Comp. Biochem. Physiol. C Toxicol. Pharmacol.* 153, 231–236. doi: 10.1016/j.cbpc.2010.11.002

Claes, J. M., and Mallefet, J. (2009a). Ontogeny of photophore pattern in the velvet belly lantern shark. Etmopterus spinax. *Zoology* 112, 433–441. doi: 10.1016/j.zool.2009.02.003

Claes, J. M., and Mallefet, J. (2009b). "Bioluminescence of sharks: first synthesis," in *Bioluminescence in Focus - A Collection of Illuminating Essays*, ed. V. Meyer Rochow (Thiruvananthapuram: Research Signpost), 51–65.

Claes, J. M., and Mallefet, J. (2009c). Hormonal control of luminescence from lantern shark (*Etmopterus spinax*) photophores. *J. Exp. Biol.* 212, 3684–3692. doi: 10.1242/jeb.034363

Claes, J. M., and Mallefet, J. (2010a). The lantern shark's light switch: turning shallow water crypsis into midwater camouflage. *Biol. Lett.* 6, 685–687. doi: 10.1098/rsbl.2010.0167

Claes, J. M., and Mallefet, J. (2010b). Functional physiology of lantern shark (*Etmopterus spinax*) luminescent pattern: differential hormonal regulation of luminous zones. *J. Exp. Biol.* 213, 1852–1858. doi: 10.1242/jeb.041947

Claes, J. M., and Mallefet, J. (2015). Comparative control of luminescence in sharks: new insights from the slendertail lanternshark (*Etmopterus molleri*). *J. Exp. Mar. Biol. Ecol.* 467, 87–94. doi: 10.1016/j.jembe.2015.03.008

Claes, J. M., Nilsson, D. E., Mallefet, J., and Straube, N. (2015). The presence of lateral photophores correlates with increased speciation in deep-sea bioluminescent sharks. *Royal Soc. Open Sci.* 2:150219. doi: 10.1098/rsos.150219

Claes, J. M., Nilsson, D. E., Straube, N., Collin, S. P., and Mallefet, J. (2014a). Iso-luminance counterillumination drove bioluminescent shark radiation. *Sci. Rep.* 4:4328. doi: 10.1038/srep04328

Claes, J. M., Partridge, J. C., Hart, N. S., Garza-Gisholt, E., Ho, H. C., Mallefet, J., et al. (2014b). Photon hunting in the twilight zone: visual features of mesopelagic bioluminescent sharks. *PLoS One* 9:e104213. doi: 10.1371/journal.pone.0104213

Claes, J. M., Sato, K., and Mallefet, J. (2011b). Morphology and control of photogenic structures in a rare dwarf pelagic lantern shark (*Etmopterus splendidus*). *J. Exp. Mar. Biol. Ecol.* 406, 1–5. doi: 10.1016/j.jembe.2011.05.033

Clarke, W. D. (1963). Function of bioluminescence in mesopelagic organisms. *Nature* 198, 1244–1246. doi: 10.1038/1981244a0

Compagno, L. J. V. (1984). Sharks of the world. an annoted and illustrated catalogue of shark species known to date. *FAO Fisher. Sympos.* 125:249.

Delroisse, J., Duchatelet, L., Flammang, P., and Mallefet, J. (2021). Photophore distribution and enzymatic diversity within the photogenic integument of the cookie cutter shark *Isistius brasiliensis* (Chondrichthyes: Dalatiidae). *Front. Mar. Sci.*

Douglas, R. H., Partridge, J. C., and Marshall, N. J. (1998). The eyes of deep-sea fish I: lens pigmentation, tapeta and visual pigments. *Prog. Retin. Eye Res.* 17, 597–636. doi: 10.1016/S1350-9462(98)00002-0

Duchatelet, L., Delroisse, J., Flammang, P., Mahillon, J., and Mallefet, J. (2019a). *Etmopterus spinax*, the velvet belly lanternshark, does not use bacterial luminescence. *Acta Histochem.* 121, 516–521. doi: 10.1016/j.acthis.2019.04.010

Duchatelet, L., Delroisse, J., and Mallefet, J. (2020a). Bioluminescence in lanternsharks: Insight from hormone receptor localization. *Gen. Comp. Endocrinol.* 294:113488. doi: 10.1016/j.ygcen.2020.113488

Duchatelet, L., Delroisse, J., Pinte, N., Sato, K., Ho, H. C., and Mallefet, J. (2020b). Adrenocorticotropic hormone and cyclic adenosine monophosphate are involved in the control of shark bioluminescence. *Photochem. Photobiol.* 96, 37–45. doi: 10.1111/php.13154

Duchatelet, L., Marion, R., and Mallefet, J. (2021). A third luminous shark family: confirmations of luminescence ability for *Zameus squamulosus* (Squaliformes; Somniodidae). *Photochem. Photobiol.* doi: 10.1111/php13393 [Epub ahead of print].

Duchatelet, L., Oury, N., Mallefet, J., and Magalon, H. (2020c). In the intimacy of the darkness: genetic polyandry in deep-sea luminescent lanternsharks *Etmopterus spinax* and *Etmopterus molleri* (Squaliformes, Etmopteridae). *J. Fish. Biol.* 96, 1523–1529. doi: 10.1111/jfb.14336

Duchatelet, L., Pinte, N., Tomita, T., Sato, K., and Mallefet, J. (2019b). Etmopteridae bioluminescence: dorsal pattern specificity and aposematic use. *Zool. Lett.* 5:9. doi: 10.1186/s40851-019-0126-2

Duchatelet, L., Sugihara, T., Delroisse, J., Koyanagi, M., Rezsohazy, R., Terakita, A., et al. (2020d). From extraocular photoreception to pigment movement regulation: a new control mechanism of the lanternshark luminescence. *Sci. Rep.* 10:10195. doi: 10.1038/s41598-020-67287-w

Dunn, M. R., Szabo, A., McVeagh, M. S., and Smith, P. J. (2010). The diet of deepwater sharks and the benefits of using DNA identification of prey. *Deep Sea Res.* 57(Pt I), 923–930. doi: 10.1016/j.dsr.2010.02.006

Ferrón, H. G., Paredes-Aliaga, M. V., Martínez-Pérez, C., and Botella, H. (2018). Bioluminescent-like squamation in the galeomorph shark *Apristurus ampliceps* (Chondrichthyes: Elasmobranchii). *Contrib. Zool.* 87, 187–196. doi: 10.1163/18759866-08703004

Haddock, S. H. D., Moline, M. A., and Case, J. F. (2010). Bioluminescence in the sea. *Annu. Rev. Mar. Sci.* 2, 443–493. doi: 10.1146/annurev-marine-120308-081028

Hurst, R. J., Bagley, N., Chatterton, T., Hanchet, S., Schofield, K., and Vignaux, M. (1992). *Standardisation of Hoki/Middle Depth Time Series Trawl Surveys. MAF Fisheries Greta Point Internal Report No. 194*. Wellington: Draft Report Held in MAF Fisheries Great point library, 89.

Johann, L. (1899). Über eigentliche epitheliale Gebilde (Leuchtorgane) bei *Spinax niger* Aus dem zoologischen Institut der Universität Rostock. *Von. Zeitschr. Wissenschaf. Zool.* 66, 136–160.

Jones, E. C. (1971). *Isistius brasiliensis*, a squaloid shark, the probable cause of crater wounds on fishes and cetaceans. *Fish. Bull. U.S.A.* 69, 791–798.

Last, P. R., and Stevens, J. D. (1994). *Sharks and Rays of Australia*. Canberra, ACT: CSIRO, 513.

Macpherson, E. (1980). Régime alimentaire de *Galeus melastomus* Rafinesque, 1810, *Etmopterus spinax* (L., 1758), et *Scymnorhinus licha* (Bonnaterre, 1788) en Méditerranée occidentale. *Vie Milieu* 30, 139–148.

Martini, S., and Haddock, S. H. D. (2017). Quantification of bioluminescence from the surface to the deep sea demonstrates its predominance as an ecological trait. *Sci. Rep.* 7, 1–11. doi: 10.1038/srep45750

Martini, S., Kuhnz, L., Mallefet, J., and Haddock, S. H. D. (2019). Distribution and quantification of bioluminescence as an ecological trait in the deep sea benthos. *Sci. Rep.* 9, 1–11. doi: 10.1038/s41598-019-50961-z

Matallanas, J. (1982). Feeding habits of *Scymnorhinus licha* in Catalan waters. *J. Fish Biol.* 20, 155–163. doi: 10.1111/j.1095-8649.1982.tb03916.x

Muñoz-Chápuli, R., Rel Salgado, J. C., and De La Serna, J. M. (1988). Biogeography of *Isistius brasiliensis* in the North-Eastern Atlantic, inferred from crater wounds on Swordfish (*Xiphias gladius*). *J. Mar. Biol. Assoc. U. K.* 68, 315–321. doi: 10.1017/S0025315400052218

Navarro, J., López, L., Coll, M., Barría, C., and Sáez-Liante, R. (2014). Short- and long-term importance of small sharks in the diet of the rare deep-sea shark *Dalatias licha*. *Mar. Biol.* 161, 1697–1707. doi: 10.1007/s00227-014-2454-2

Nicol, J. A. (1978). "Bioluminescence and vision," in *Bioluminescence in Action*, ed. P. J. Herring (London: Academic Press), 367–408.

Ohshima, H. (1911). Some observations on the luminous organs of fishes. *J. Coll. Sci. Imp. Univ. Tokyo* 27, 1–25. doi: 10.1002/jez.1402590102

Papastamatiou, Y. P., Wetherbee, B. M., O'Sullivan, J., Goodmanlowe, G. D., and Lowe, C. G. (2010). Foraging ecology of cookiecutter sharks (*Isistius brasiliensis*) on pelagic fishes in Hawaii, inferred from prey bite wounds. *Environ. Biol. Fish.* 88, 361–368. doi: 10.1007/s10641-010-9649-2

Pinte, N., Parisot, P., Martin, U., Zintzen, V., De Vleeschouwer, C., Roberts, C. D., et al. (2020). Ecological features and swimming capabilities of deep-sea sharks from New Zealand. *Deep Sea Res.* 156:103187. doi: 10.1016/j.dsr.2019.103187

Reif, W.-E. (1985). Functions of scales and photophores in mesopelagic luminescent sharks. *Acta Zool.* 66, 111–118. doi: 10.1111/j.1463-6395.1985.tb00829.x

Renwart, M., Delroisse, J., Claes, J. M., and Mallefet, J. (2014). Ultrastructural organization of lantern shark (*Etmopterus spinax* Linnaeus, 1758) photophores. *Zoomorphology* 133, 405–416. doi: 10.1007/s00435-014-0230-y

Renwart, M., Delroisse, J., Flammang, P., Claes, J. M., and Mallefet, J. (2015). Cytological changes during luminescence production in lanternshark (*Etmopterus spinax* Linnaeus, 1758) photophores. *Zoomorphology* 134, 107–116. doi: 10.1007/s00435-014-0235-6

Renwart, M., and Mallefet, J. (2013). First study of the chemistry of the luminous system in a deep-sea shark, *Etmopterus spinax* Linnaeus, 1758 (Chondrichthyes: Etmopteridae). *J. Exp. Mar. Biol. Ecol.* 448, 214–219. doi: 10.1016/j.jembe.2013.07.010

Roberts, C. D., Stewart, A. L., and Struthers, C. D. (2015). *The Fishes of New Zealand*, Vol. 2. Wellington: Te Papa Press, 1–576.

Seigel, J. A. (1978). Revision of the dalatiid shark genus *Squaliolus*: anatomy, systematics, ecology. *Copeia* 1978, 602–614. doi: 10.2307/1443684

Shimomura, O. (2006). *Bioluminescence: Chemical Principles and Methods.* Singapore: World Scientific.

Stevens, D. W., O'Driscoll, R. L., Ballara, S. L., and Schimel, A. C. G. (2018). *Trawl Survey Of Hoki and Middle-Depth Species on the Chatham Rise, January 2018 (TAN1801). New Zealand Fisheries Assessment Report* 2018/41. Available online at: https://fs.fish.govt.nz/Doc/24639/FAR-2018-41-Trawl-Survey-TAN1801.pdf.ashx (accessed January 15, 2021).

Straube, N., Duhamel, G., GaSco, N., Kriwet, J., and Schliewen, U. K. (2011). "Description of a new deep-sea lantern shark *Etmopterus viator* sp. nov. (Squaliformes: Etmopteridae) from the Southern hemisphere," in *The kerguelen Plateau, Marine Ecosystem and Fisheries*, eds G. Duhamel., and D. Welsford (Paris: Société française d'ichtyologie), 135–148.

Straube, N., Li, C., Claes, J. M., Corrigan, S., and Naylor, G. J. P. (2015). Molecular phylogeny of squaliformes and first occurrence of bioluminescence in sharks. *BMC Evol. Biol.* 15:162. doi: 10.1186/s12862-015-0446-6

Tracey, D., and Shearer, P. (2002). *An Identification Guide for Deepwater Shark Species.* Wellington: NIWA, 16.

Warrant, E. J. (2004). Vision in the dimmest habitats on earth. *J. Comp. Physiol. A Neuroethol. Sens. Neural Behav. Physiol.* 190, 765–789. doi: 10.1007/s00359-004-0546-z

Warrant, E. J., and Locket, N. A. (2004). Vision in the deep sea. *Biol. Rev.* 79, 671–712. doi: 10.1017/S1464793103006420

Widder, E. A. (1998). A predatory use of counterillumination by the squaloid shark, *Isistius brasiliensis. Environ. Biol. Fishes* 53, 267–273. doi: 10.1023/A: 1007498915860

Widder, E. A. (1999). "Bioluminescence," in *Adaptative Mechanisms in the Ecology of Vision*, eds S. N. Archer, M. B. A. Djamgoz, E. R. Loew, J. C. Partridge., and S. Vallerga (Dordrecht: Springer). doi: 10.1007/978-94-017-0619-3-19

Zintzen, V., Roberts, C. D., Anderson, M. J., Stewart, A. L., Struthers, C. D., and Harvey, E. S. (2011). Hagfish predatory behavior and slime defence mechanism. *Sci. Rep.* 1:131.

Conflict of Interest: The authors declare that the research was conducted in the absence of any commercial or financial relationships that could be construed as a potential conflict of interest.